The Effect of Bicyclo[2.2.1]hept-5-ene-2,3-dicarboxylate on the Mechanical Properties and Crystallization Behaviors of Isotactic Polypropylene

Zhi Cai, Shicheng Zhao, Benxian Shen, Zhong Xin

State-Key Laboratory of Chemical Engineering and Department of Product Engineering, East China University of Science and Technology, Shanghai 200237, People's Republic of China

Received 13 June 2009; accepted 22 September 2009
DOI 10.1002/app.31486
Published online 10 Decemebr 2009 in Wiley InterScience (www.interscience.wiley.com).

ABSTRACT: The mechanical and optical properties of iPP nucleated with bicyclo[2.2.1]heptenedicarboxylate salts (BCHED) have been investigated. The results showed that aluminum bicyclo[2.2.1]heptenedicarboxylate (BCHE13) is the most effective nucleating agent to improve the mechanical and optical properties. Then the effects of the BCHE13 concentration on mechanical and optical properties and crystallization behaviors were studied. The results indicated that the saturated concentration of BCHE13 is about 0.2 wt %, at which nucleated iPP showed the better comprehensive mechanical and optical properties and high crystallization peak temperature. Nonisothermal crystallization kinetics of iPP nucleated with different BCHE13 contents have been investigated by Caze method. The results indicated Avrami exponents of nucleated iPP gradually increased with the increasing of BCHE13 concentration. The results can be explained that crystallization and growth model of nucleated iPP is heterogeneous nuclei followed by more than three-dimension spherical growth during nonisothermal crystallization, which can be proved by agglomeration of BCHE13 in melt iPP. © 2009 Wiley Periodicals, Inc. J Appl Polym Sci 116: 792–800, 2010

Key words: isotactic polypropylene; nucleating agent; crystallization kinetics; bicyclo[2.2.1]heptenedicarboxylate salt

INTRODUCTION

The crystallization of isotactic polypropylene (iPP) is generally described in terms of a crystalline nucleation and growth model, and the rate of nucleation determines the rate of overall crystallization.[1] It is assumed that nuclei form from ordered segments as a result of thermal fluctuations in the melt and then these nuclei grow by the addition of more segments until a stable crystalline structure develops. The addition of nucleating agents can accelerate the process of crystalline nucleation by providing massive foreign nucleation sites. Up to now, the use of nucleating agents in iPP is widespread and of great commercial importance because the control of the crystallization process allows one to modify the optical, mechanical and processing properties of iPP.

A large number of compounds have been reported to induce the α-form of iPP.[2–13] These nucleating agents are mainly categorized into three types by the structure: (1) sorbitol derivatives,[2–4] such as 1,3 : 2,4-dibenzylidenesorbitol (DBS, Millad 3905, Milliken Chemical and Irgaclear D, Ciba speciality Chemicals), bis(3,4-dimethybenzylidene)-sorbitol (DMDBS, Millad 3988); (2) organic phosphate derivatives,[5–12] such as sodium 2,2-methylene-bis(4,6-di-tert-butylphenyl)-phosphate (commercial product name: ADK STAB NA-11) and aluminum salt of 2,2-methylene-bis(4,6-di-tert-butylphenyl)phosphate (commercial product name: ADK STAB NA-21); (3) organic carboxylic acid salt,[12–14] such as sodium benzoate and salts of dehydroabietic acid. The effects of these nucleating agents on crystallization behavior and kinetics of iPP has been extensively investigated.[2–14] However, the effects of organic dicarboxylic acid salts acting as α nucleating agent on mechanical properties and crystallization behavior of iPP are rarely studied.[14] It was reported that bicyclo[2.2.1]hept-5-ene-2,3-dicarboxylate salts (BCHED) are effective nucleating agents.[15] Especially, it exhibits significantly higher polymer crystallization peak temperature, shorter crystallization halftime. So far, the mechanical and optical properties of iPP nucleated with the nucleators and the concentration effect of the nucleating agents were not reported. In our previous work, the crystallization kinetics of iPP nucleated by BCHED has been investigated,[16] but the effect of the concentration of the nucleating agent on nonisothermal crystallization kinetics has not been discussed.

In this article, the effects of BCHED on the mechanical and optical properties and the crystallization

Correspondence to: Z. Xin (xzh@ecust.edu.cn).
Contract grant sponsor: National Natural Science Foundation of China; contract grant number: 20876042.

behaviors of iPP were investigated. And then the effects of the concentration of aluminum salt bicyclo[2.2.1]heptenedicarboxylate (BCHE13) on the mechanical and optical properties, and crystallization behaviors were further studied. The nonisothermal crystallization experiments of virgin iPP and nucleated iPP with different BCHE13 content were carried out by differential scanning calorimetry (DSC). Caze method[17] was chosen to describe the nonisothermal crystallization kinetics as it can avoid selecting the zero point of crystallization. While other methods, such as Jeziorny method,[18] Ozawa method,[19] and Mo method[20] involve the zero point selection, which has obvious effect on the calculated results.

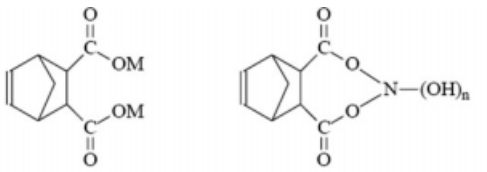

Name	BCHE03	BCHE11	BCHE19	Name	BCHE12	BCHE20	BCHE13
M	Li	Na	K	N	Mg	Ca	Al
				n	0	0	1

Scheme 1 The chemical structure of nucleating agents in this study.

EXPERIMENTAL

Materials

The iPP powder (T30S) used in this study was kindly provided by Jiujiang petrochemical Corporation (China). The material has a melt flow index of 3.4 g/10 min. The nucleating agents are metal salts of BCHED, and their structures are shown in Scheme 1. BCHED were synthesized by hydrothermal method according to literature.[15] These nucleating agents were white powder and their melting points are above 300°C.

Sample preparation

The nucleating agent (0.2 wt %) and antioxidant (0.1 wt %) were added into the iPP powders then mixed in a high-speed mixer for 5 min. The mixture was extruded by an SJSH-30 twin-screw extruder through a strand die and palletized for DSC measurement.

Mechanical properties

The mechanical properties were measured according to ASTM test methods, such as D-638 for the tensile properties and D-790 for the flexural properties, using a universal testing machine. The Izod impact strength was tested on the basis of D-256.

Apparatus and experimental procedures

A perkinelmer Diamond DSC (PerkinElmer Company, USA) was used for calorimetric investigations of nonisothermal crystallization. Calibration was performed using pure indium at a heating rate of 20 K/min. All DSC operations were carried out under a nitrogen environment. The sample weights were approximately 3 mg and all samples were heated to 473 K and hold in the molten state for 5 min to eliminate the thermal history. Nonisothermal crystallization experiments were carried out by cooling samples from 473 K to 323 K using different cooling rates. The exotherms were recorded with the cooling rates 2.5, 5, 10, 15, 20 K/min, respectively.

Polarized optical microscopy (POM)

The morphology studies of pure iPP and nucleated iPP were performed with the aid of an Olympus BX51 (Japan) polarized optical microscopy attached with a DP70 digital camera, and a THMS600 hot-stage. Extruded sample were placed between two microscopy slides, melted and pressed at 473 K for 5 min to erase any trace of crystal, and then rapidly cooled to a predetermined crystallization temperature. The samples were kept isothermal until the crystallization process was completed, and meanwhile, photographs were automatically taken.

Theory of crystallization

The Avrami equation[21,22] is widely used to describe the polymer isothermal crystallization.

$$X_t = 1 - \exp(-Z(T)t^n) \tag{1}$$

where X_t is the relative crystallinity at time t, n is a constant whose value depends on the mechanism of nucleation and on the form of crystal growth, and $Z(T)$ is a constant containing the nucleation and growth parameters.

Crystallization halftime ($t_{1/2}$), defined as the time to a relative crystallinity of 50%, can be obtained:

$$t_{1/2} = \left(\frac{\ln 2}{Z(T)}\right)^{1/n} \tag{2}$$

The time at maximum heat flow (t_{max}) can be calculated by:

$$t_{max} = [(n-1)/nZ(T)]^{1/n} \tag{3}$$

The Avrami equation has been extended by Ozawa to develop a simple method to study the

TABLE I
The Effect of Different Nucleating Agents on Mechanical and Optical Properties of iPP

Properties	Tensile strength/MPa	Tensile modulus/MPa	Flexural strength/MPa	Flexural modulus/MPa	Impact strength/(J.m^{-1})	Haze value/%
iPP	37.0	1109.5	43.0	1361.0	31.6	81.1
iPP/BCHE03	38.67	1321.5	45.3	1445.4	30.5	77.8
iPP/BCHE11	39.05	1326.7	45.2	1566.0	30.2	68.9
iPP/BCHE19	38.34	1293.1	43.9	1410.1	30.6	79.8
iPP/BCHE20	38.68	1310.6	49.2	1540.3	30.3	72.0
iPP/BCHE12	37.32	1154.6	43.8	1397.6	31.5	80.2
iPP/BCHE13	39.32	1319.8	53.0	1767.4	29.3	51.0

nonisothermal experiment. The general form of Ozawa theory is written as follows:

$$X_v(T) = 1 - \exp(-K_T/\phi^m) \quad (4)$$

where K_T is the cooling crystallization function, Φ is the cooling rate, and m is the Ozawa exponent that depends on the dimension of the crystal growth. In Ozawa method, there is a main hypothesis that n is independent of temperature and only a limited number of X_v data are available for the foregoing analysis, as the onset of crystallization varies considerably with the cooling rate.

Caze et al.[17] put forward a new method to modify Ozawa equation. It was assumed an exponential increase of K_T with T upon cooling. On the basis, the temperature at the peak and the two inflection points of the exotherm with skew Gaussian shape are linearly related to lnΦ in order to estimate the exponent n.

On the basis of the findings on the crystallization behavior of poly(ethylene terephthalate) and PP, Kim et al.[23] proposed

$$\ln K_T = a(T - T_1) \quad (5)$$

where a and T_1 are empirical constants. If the extreme point of the pertinent $\partial X_v(T)/\partial T$ curve occurs at $T = T_q$ (crystallization peak temperature), i.e. $(\partial^2 X_v(T)/\partial T^2)_{Tq} = 0$, we have:

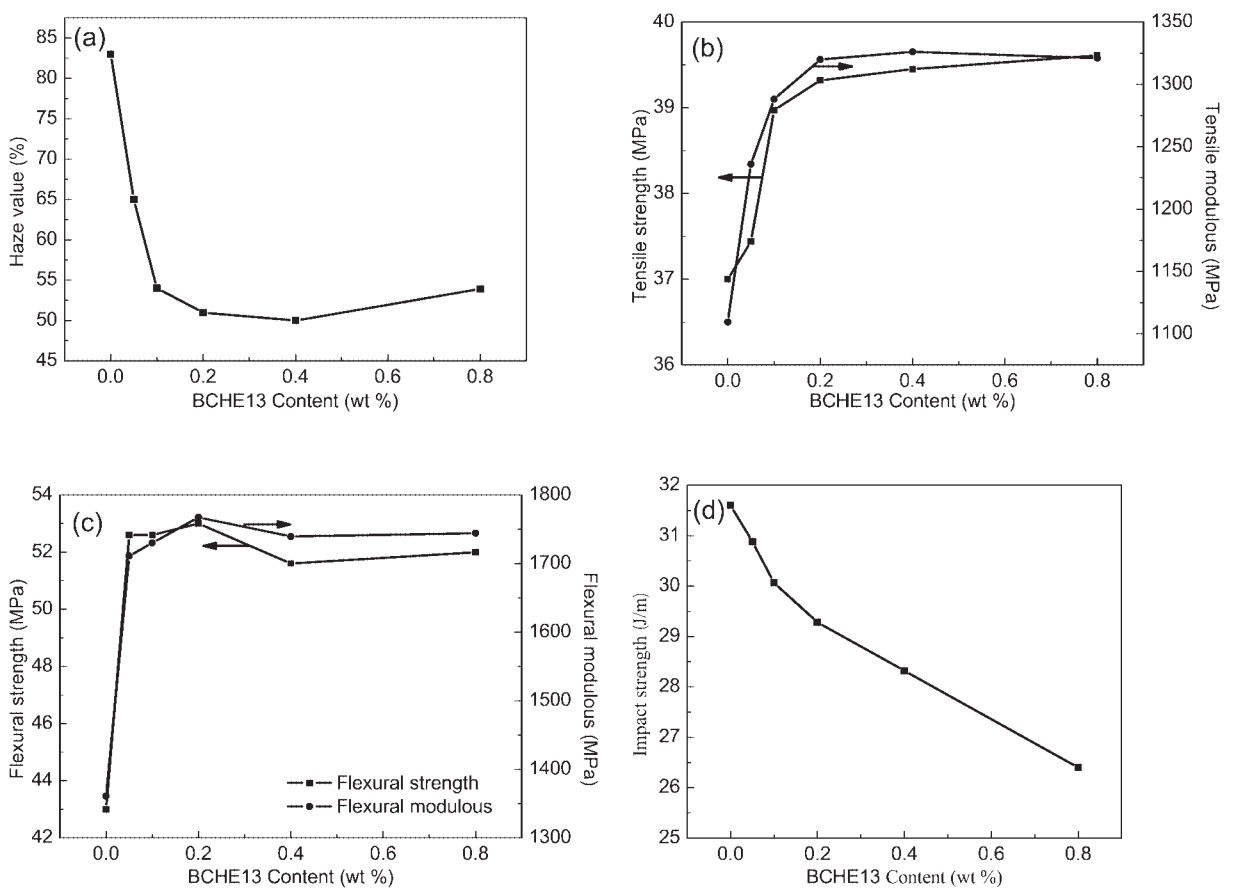

Figure 1 Mechanical and optical properties of iPP nucleated by the different BCHE13 content.

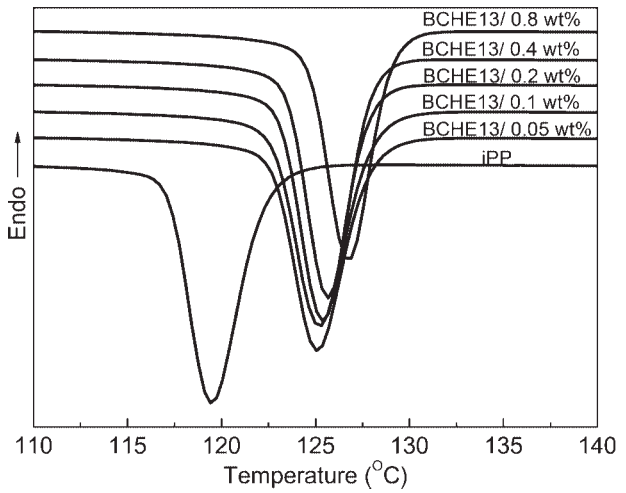

Figure 2 The crystallization curves of iPP samples with different BCHE13 contents at the cooling rate 20°C/min.

$$K_T(T_q) = \phi^n \tag{6}$$

Combining eqs. (4)–(6) yields:

$$\ln[-\ln(1 - X_v(T))] = a(T - T_q) \tag{7}$$

Hence, a linear plot of $\ln[-\ln(1 - X_v(T))]$ vs. T would result in the constant a and the product $-aT_q$ from the gradient and intercept, respectively. At $T = T_q$, obtained from the foregoing algorithm, eqs. (6) and (7) lead to:

$$T_q = n \ln \phi / a + T_1 \tag{8}$$

As such, parameter n can be obtained from the linear plot of T_q vs. $\ln\Phi/a$ in accordance with eq. (8).

RESULTS AND DISCUSSION

The effect of BCHED on mechanical and optical properties of iPP

The mechanical and optical properties of iPP nucleated by the Li, Na, K, Ca, Mg, Al salts of bicyclo[2.2.1]heptenedicarboxylate were characterized and the results were listed in Table I. From the Table I, it can be seen that BCHED can significantly increase the tensile and flexural properties, however, decrease the impact strength of iPP. The haze values of nucleated iPP obviously decrease compared with that of virgin iPP. BCHE13 showed the best nucleation effect among all the BCHED. The tensile strength and flexural modulus increase 6.2% and 29.9% compared with those of virgin iPP, respectively. The haze vale decrease 37.1% with that of virgin iPP. So it is necessary to further investigate the effects of the content of BCHE13 on the mechanical, optical properties, and crystallization behaviors.

The effect of BCHE13 concentration on mechanical and optical properties of iPP

The mechanical and optical properties of iPP nucleated different content BCHE13 are shown in Figure 1. From Figure 1(a), it can be seen that haze values of iPP nucleated by BCHE13 first significantly decreased and then gradually increased. When the content of BCHE13 is 0.2–0.4 wt %, the haze value reaches the lowest (about 60% of pure iPP). From the Figure 1(b,c), it can be seen that tensile and flexural properties increase rapidly when BCHE13 is less than 0.2 wt %, and then basically keep constant with the further increase of BCHE13. When the content of BCHE13 is 0.2 wt %, the tensile strength and flexural modulus of nucleated iPP improved about 6.2% and 29.9% compared with that of pure iPP, respectively. The impact strength of iPP nucleated by BCHE13 gradually decrease with the content. Therefore, the 0.2 wt % BCHE13 is better in the industry application considering the comprehensive mechanical and optical properties and cost.

The effect of BCHE13 concentration on crystallization behavior

To check the effect of the nucleating agent BCHE13 on crystallization behavior, the crystallization curves of iPP with different BCHE13 contents are plotted in Figure 2. For the pure iPP, the T_p is around 119°C. The T_p of the nucleated iPP by 0.05 wt % BCHE13 is about $T_p = 125$°C. With the increasing of BCHE13 contents, the crystallization peak temperature of iPP shift to higher temperature. Figure 3 shows a plot of crystallization peak temperature as a function of BCHE13 contents, from which we can see that the increase of T_p is very strong when the contents of BCHE13 is lower than 0.05 wt %, while that is weak when the contents of BCHE30 is higher than 0.2 wt %. T_p (125.6°C) of iPP nucleated with 0.2 wt % BCHE13 is higher than that (119.4°C) of the pure iPP

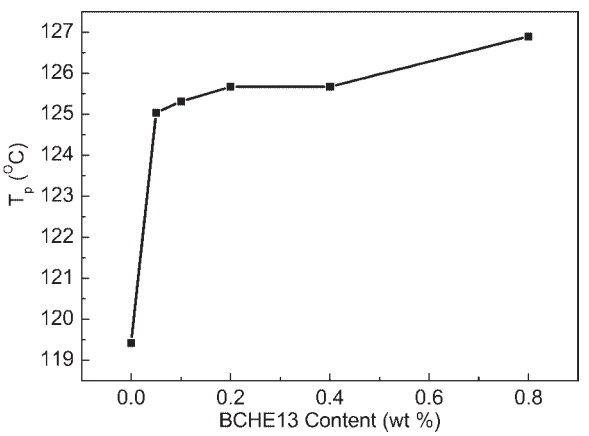

Figure 3 T_p as a function of BCHE13 contents.

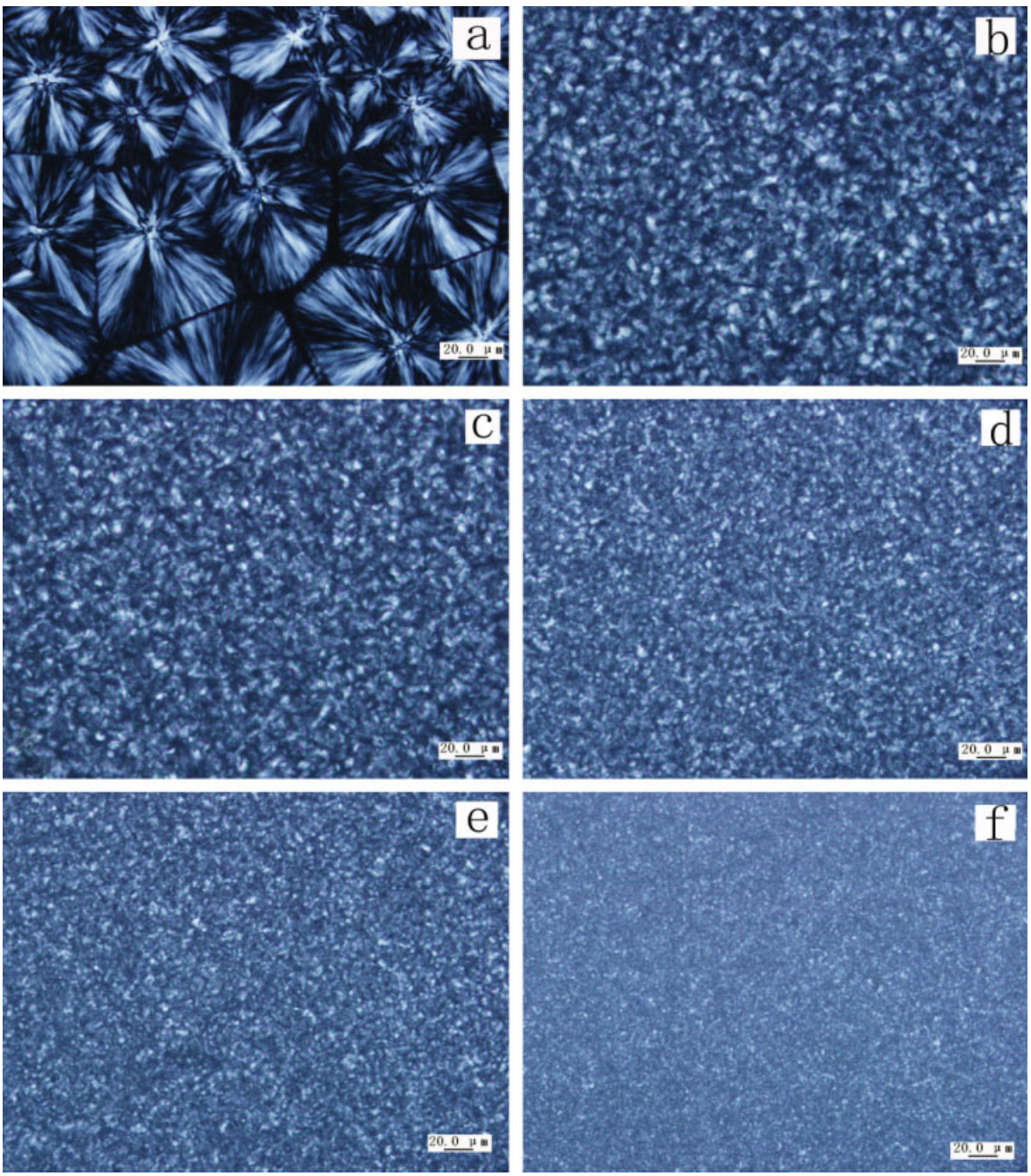

Figure 4 Polarized optical micrographs of iPP (a), nucleated iPP with different BCHE13 concentration 0.05 wt % (b), 0.1 wt % (c), 0.2 wt % (d), 0.4 wt % (e), 0.8 wt % (f) under isothermal crystallization at 140°C. [Color figure can be viewed in the online issue, which is available at www.interscience.wiley.com.]

by 6.2°C. It indicates that 0.2 wt % is the saturated concentration and more nucleating agent is less effective in increasing the crystallization peak temperature further.

Polarized optical micrographs of pure iPP and nucleated iPP with different concentrations of BCHE13 crystallized under isothermal conditions are shown in Figure 4. For the pure iPP, the spherulite diameter is more than 20 mm. The incorporation of BCHE13 greatly decreases the spherulite size even the content is low. Furthermore, the spherulite size decrease greatly before the concentration of nucleating agent reaches 0.2 wt % and then decrease slightly with a further increase of BCHE13. This is in good agreement with the result of crystallization peak temperature. As we know that the crystallization process includes the nucleation and the crystal growth. In pure iPP, the forming of nuclei is difficult; spherulite growth is mainly homogeneous nucleation, followed by nucleation-controlled

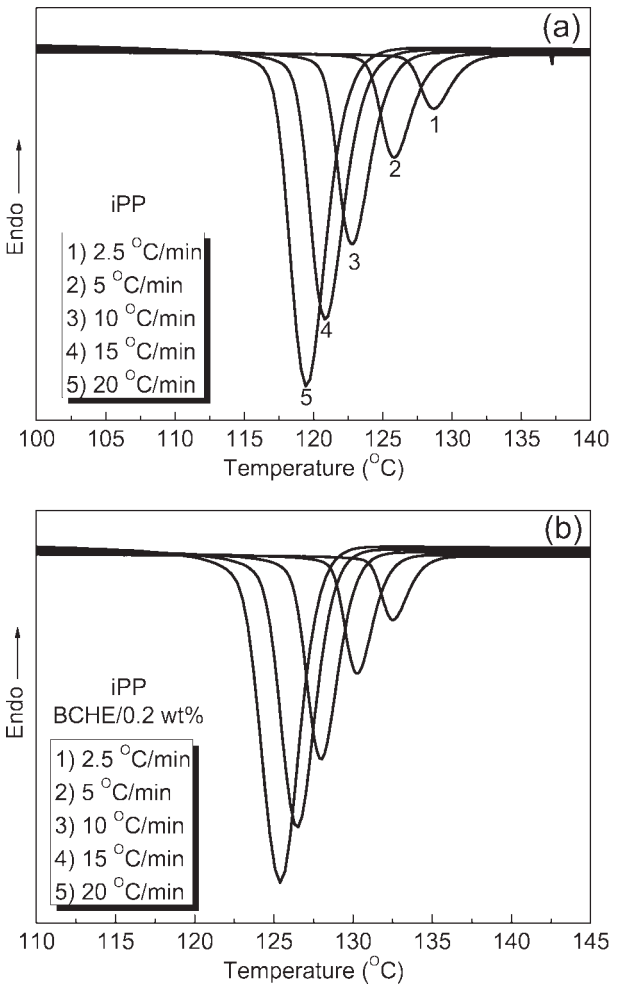

Figure 5 DSC cooling curves of (a) iPP and (b) iPP/(BCHE13/0.2 wt %) at different cooling rates.

spherulite growth. As the nucleation rate is slow and number of nucleus is very few, the spherulite of iPP can become very large before it impinges another spherulite. While in nucleated iPP, a large number of nuclei should be produced because of the existence of nucleating agents, and so the nucleation rate is very fast and the spherulite growth in it is heterogeneous nucleation, followed by diffusion-controlled growth. Because of the existence of a great deal of nuclei, the spherulite can not grow large enough to overlap, and so the size of spherulites in nucleated iPP should be much smaller than those in pure iPP.

The effect of BCHE13 concentration on nonisothermal crystallization kinetics

Crystallization process of semi-crystalline polymers can have a dramatic impact on the mechanical properties and hence is important to final application. Practical processes usually proceed under nonisothermal crystallization conditions. In order to find the optimum conditions in the industrial process and obtain products with better properties, it is necessary to have quantitative evaluations on the nonisothermal crystallization process; therefore the study of nonisothermal crystallization kinetics has great practical importance. Furthermore, the effect of nucleating agent concentration on the nonisothermal crystallization kinetics was not reported. Therefore, the nonisothermal crystallization of iPP and iPP nucleated by different content BCHE13 was carried out by DSC with cooling rates from 2.5°C/ min to 20°C/ min. The thermograms of neat iPP and iPP/BCHE13 (0.2 wt %) are plotted in Figure 5. Those of nucleated iPP with other concentration are similar with that of iPP/BCHE13 (0.2 wt %). It is evident that the crystallization temperature is affected by the cooling rate. The higher is the cooling rate; the lower is the crystallization peak temperature. Furthermore, it can be recognized that, at the same cooling rates, T_{cp} of nucleated iPP is greatly increased compared with virgin iPP.

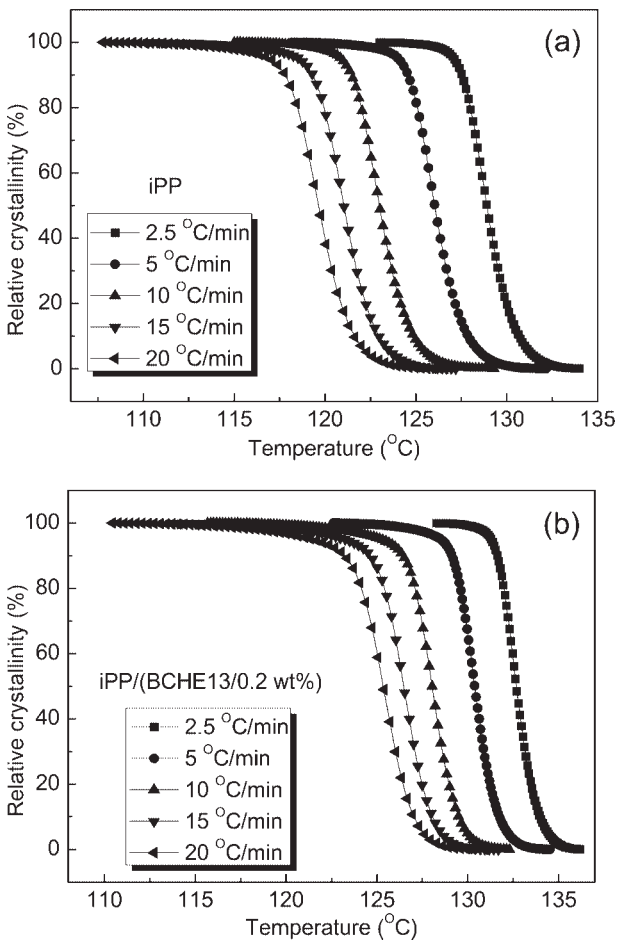

Figure 6 Relative crystallinity of (a) virgin iPP and (b) iPP/(BCHE13/0.2 wt %) at different cooling rates.

TABLE II
Parameters of NonIsothermal Crystallization Kinetics for iPP and iPP with Different BCHE13 Contents Obtained by Caze Method

Sample	Φ, °C/min	T_p[a] (°C)	$t_{1/2}$, s	a	T_q[b] (°C)	n
iPP	2.5	128.7	122.6	−1.22	128.6	4.41 ± 0.11
	5	125.8	73.6	−1.11	125.7	
	10	122.7	37.8	−1.09	122.7	
	15	120.8	24.6	−1.08	120.7	
	20	119.4	20.9	−1.03	119.3	
0.05 wt %	2.5	131.5	104.2	−1.56	131.4	2.98 ± 0.09
	5	129.7	57.6	−1.41	129.6	
	10	127.5	32.0	−1.24	127.3	
	15	126.2	26.6	−1.13	125.9	
	20	125.0	19.3	−1.06	124.8	
0.1 wt %	2.5	132.0	91.7	−1.64	132.0	2.97 ± 0.13
	5	129.9	53.8	−1.48	129.9	
	10	127.8	34.7	−1.21	127.6	
	15	126.5	25.8	−1.10	126.1	
	20	125.3	21.9	−1.03	124.8	
0.2 wt %	2.5	132.2	84.5	−1.70	132.5	4.10 ± 0.21
	5	130.4	49.6	−1.57	130.2	
	10	128.1	25.6	−1.50	127.8	
	15	126.7	20.8	−1.35	126.2	
	20	125.7	16.7	−1.27	125.0	
0.4 wt %	2.5	132.2	97.9	−1.57	132.2	4.22 ± 0.05
	5	130.4	54.1	−1.55	130.3	
	10	128.1	28.6	−1.46	127.9	
	15	126.7	20.2	−1.39	126.5	
	20	125.7	15.8	−1.36	125.4	
0.8 wt %	2.5	135.0	117.6	−1.35	134.9	5.22 ± 0.12
	5	132.2	53.8	−1.40	132.1	
	10	129.6	31.3	−1.34	129.3	
	15	127.9	22.6	−1.34	127.7	
	20	126.9	16.3	−1.30	126.4	

[a] Determined from Fig. 5.
[b] Calculated from Caze method.

By means of integrating the partial areas under the DSC endotherm, it can be obtained the values of the crystalline weight fraction X_w (T) (Fig. 6).

Crystallization halftime$t_{1/2}$ can be obtained from Figure 6 by using equation $t = (T_0 - T)/\phi$ (where t is the crystallization time, T_0 is the onset crystallization temperature, T is the crystallization temperature at $X_w(T) = 50\%$ and Φ is the cooling rate). The results are listed in Table II. It can be seen that the addition of BCHE13 can obviously shorten $t_{1/2}$ of iPP, especially at low cooling rate. When the cooling rate is 2.5°C/min, $t_{1/2}$ of pure iPP is 122.6 s while that of iPP/BCHE13 (0.2 wt %) is 84.5 s.

Now X_w (T) can be converted into X_v (T) by eq. (14)[22]:

$$X_v(T) = \frac{X_w(T)\frac{\rho_a}{\rho_c}}{1 - \left(1 - \rho_a \Big/ \rho_c\right) X_w(T)} \qquad (14)$$

where ρ_a and ρ_c are the bulk densities of the polymer in the amorphous and pure crystalline states,

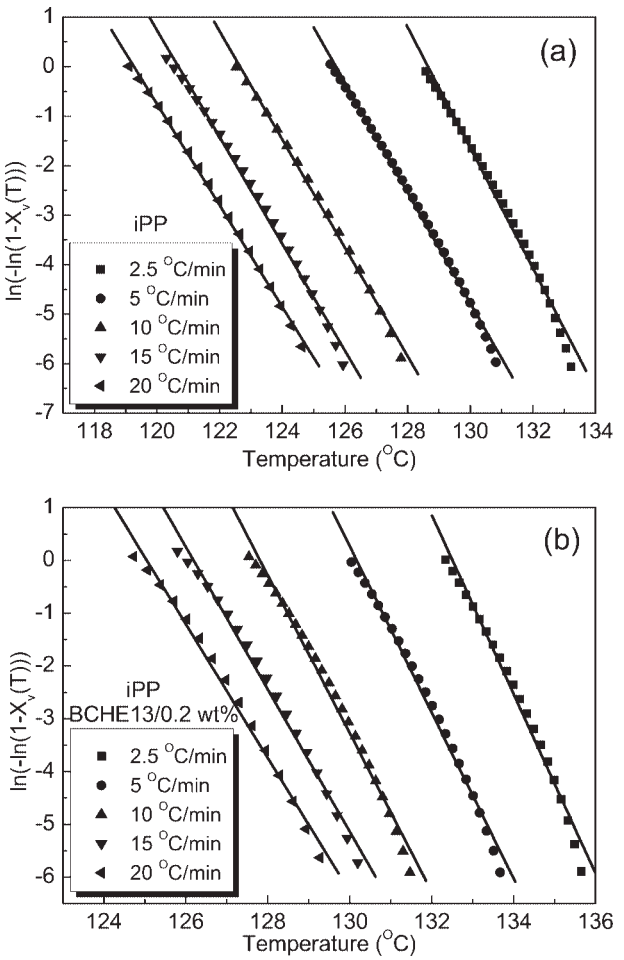

Figure 7 Plots of ln[−ln(1 − $X_v(T)$)] versus T for (a) virgin iPP and (b) iPP/(BCHE13/0.2 wt %).

respectively. For iPP, the density of the amorphous phase (ρ_a) is 0.852, and that of the crystallized phase (ρ_c) is 0.935. Therefore, plots of ln[−ln(1 − $X_v(T)$)] vs. T are shown in Figure 7 and there is good linear relationship in the initial crystallization stage. The values of a and $-aTq$ can be determined from the

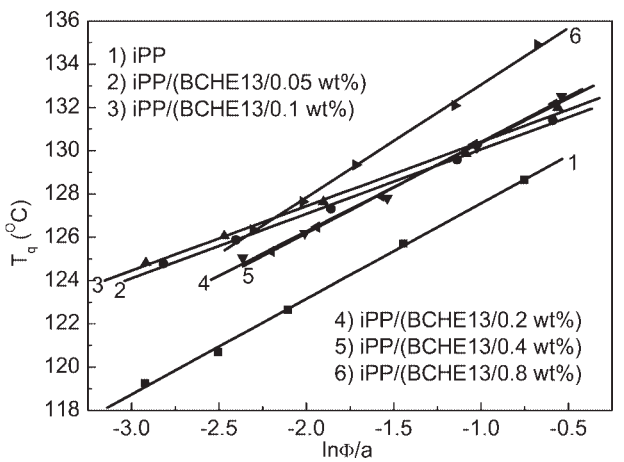

Figure 8 Plots of T_q vs. lnΦ/a for iPP and nucleated iPP.

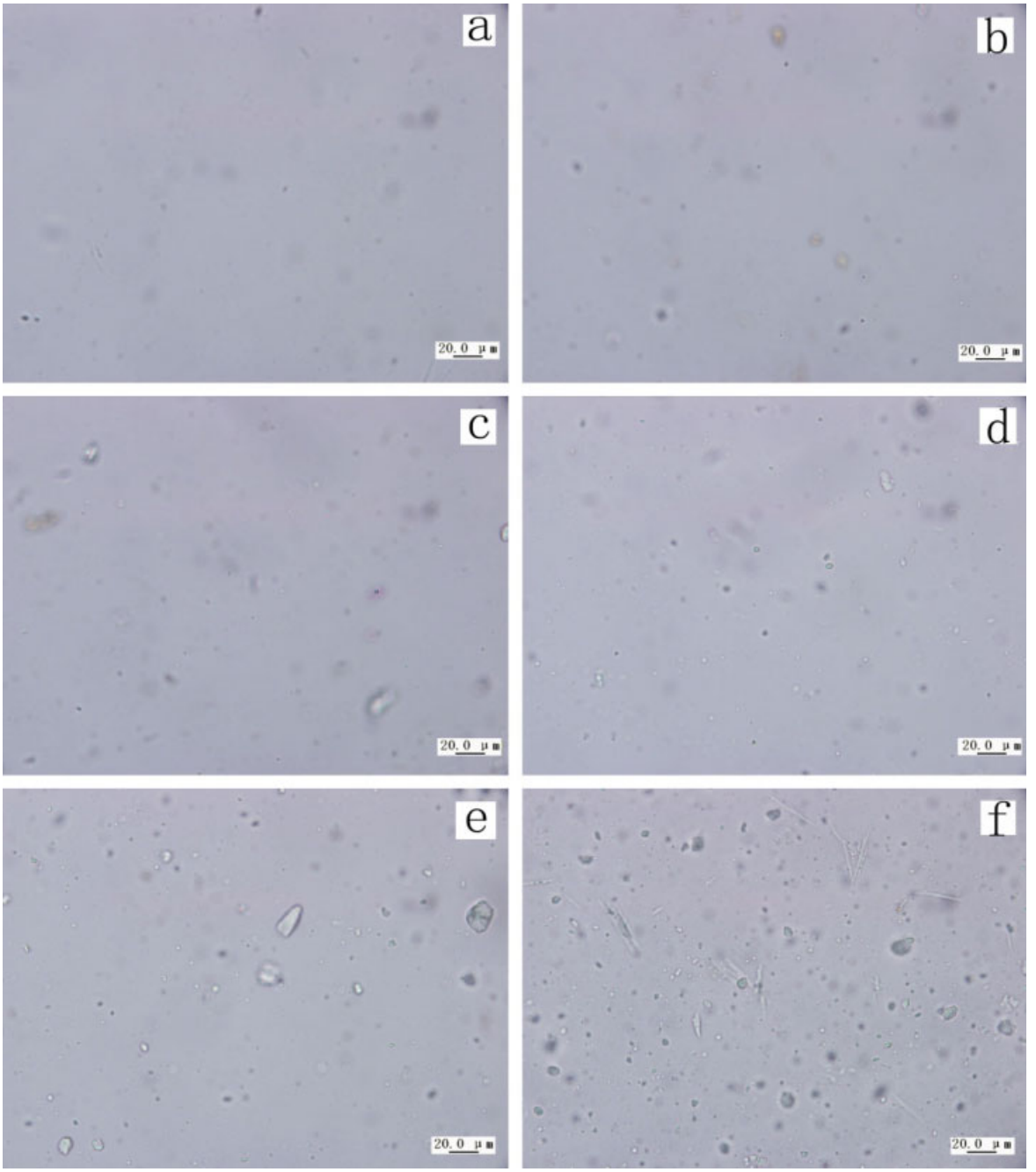

Figure 9 The morphology of nucleating agents BCHE13 in melting iPP (200°C); the content of nucleating agent is 0 wt % (a), 0.05 wt % (b), 0.1 wt % (c), 0.2 wt % (d), 0.4 wt % (e), 0.8 wt % (f), respectively. [Color figure can be viewed in the online issue, which is available at www.interscience.wiley.com.]

slope and intercept of each straight line, and the results are also listed in Table II.

Straight lines can be obtained from plots of obtained T_q vs. $\ln\Phi/a$ under different cooling rates (Fig. 8), and good linearity of those curves suggests that the Caze model works well in describing the nonisothermal crystallization for iPP and nucleated iPP. Avrami exponents of iPP and nucleated iPP can be determined from the slope of each straight line and the results are also listed in Table II.

From the results presented in Table II, it is evident that crystallization peak temperature obtained from the experimental data is in agreement with that from Caze method, indicating the validity of Caze method. The crystallization peak temperatures of nucleated iPP are higher than those of pure iPP for the same cooling rate, which reveals that nucleating agents act as nucleation sites and accelerate the crystallization of iPP. For pure iPP, the Avrami exponent is 4.41, corresponding to three-dimensional spherical

growth and thermal nucleation in the primary crystallization stage. However, Avrami exponents of nucleated iPP are obviously influenced by the content of BCHE13. With the increase of BCHE13 content, Avrami exponents of nucleated iPP gradually increase. When the content of BCHE13 is 0.05, 0.1, 0.2, 0.4, 0.8 wt %, the n values of nucleated iPP are 2.98, 2.97, 4.10, 4.22, and 5.22, respectively. When the content of BCHE13 is lower than 0.2 wt %, the n values of nucleated iPP is about 3, which shows that crystallization and growth model of nucleated iPP is heterogeneous nuclei followed by three-dimension spherical growth during nonisothermal crystallization. When the content of BCHE13 is higher than 0.2 wt %, the n value of nucleated iPP is larger than 4. The result can be explained that crystallization and growth model of nucleated iPP is heterogeneous nuclei followed by more than three-dimension spherical growth during nonisothermal crystallization, which can be proved by the morphology of nucleating agents with different contents. The morphology of nucleating agents in melting iPP is characterized by POM, which are shown in Figure 9. From Figure 9, it can be seen that the agglomeration of nucleating agents is not obvious when the content of BCHE13 is lower than 0.2 wt %, while the agglomeration of BCHE13 is more obvious with the increase of BCHE13 content. However, the correlation between the Avrami parameter and the agglomeration of nucleating agent still need more direct evidence and more explanation. This will be studied in detail in the following work.

CONCLUSION

The mechanical and optical properties of iPP nucleated with bicyclo[2.2.1]heptenedicarboxylate salts (BCHED) have been investigated. The results showed that aluminum salt bicyclo[2.2.1]heptene dicarboxylate (BCHE13) is the most effective nucleating agent to improve the mechanical and optical properties. The effects of the BCHE13 concentration on mechanical and optical properties of iPP were studied. The results indicated the tensile and flexural properties of nucleated iPP first increase and then basically keep constant while haze values of nucleated iPP first decrease and then gradually increase with the BCHE13 contents. The saturated concentration of BCHE13 is about 0.2 wt %, at which nucleated iPP showed the better comprehensive mechanical and optical properties. The crystallization behavior was studied by DSC and POM. It shows that BCHE13 can greatly increase the crystallization peak temperature of iPP and sharply decreases the spherulite sizes of iPP with the increasing of the content of BCHE13. Nonisothermal crystallization kinetics of iPP nucleated with different BCHE13 contents has been investigated by Caze method. The results indicate Avrami exponents of nucleated iPP gradually increase from 3 to 5 with the increase of BCHE13 concentration. The results can be explained that crystallization and growth model of nucleated iPP is heterogeneous nuclei followed by more than three-dimension spherical growth during nonisothermal crystallization, which can be proved by agglomeration of BCHE13 in melt iPP.

References

1. Mandelkern, L. In Comprehensive Polymer Science;Allen, G., Bevington, J., Eds.; Polymer Properties; Pergamon Press: New-York, 1989; Vol. 2, in Eds.
2. Jin, Y.; Hiltner, A.; Baer, E. J Polym Sci Part B: Polym Phys 2007, 45, 1788.
3. Kristiansen, M.; Werner, M.; Tervoort, T.; Smith, P. Macromolecules 2003, 36, 5150.
4. Marco, C.; Ellis, G.; Gómez, M. A.; Arribas, J. M. J Appl Polym Sci 2002, 84, 2440.
5. Zhang, G. P.; Yu, J. Y.; Xin, Z.; Gui, Q. D.; Wang, S. Y. J Macromol Sci Phys 2003, 42, 663.
6. Zhang, Y.-F.; Xin, Z. J Appl Polym Sci 2006, 101, 3307.
7. Mai, K. C.; Wang, K. F.; Han, Z. W.; Zeng, H. M. J Appl Polym Sci 2001, 81, 78.
8. Yoshimoto, S.; Ueda, T.; Yamanaka, K.; Kawaguchi, A.; Tobita, E.; Haruna, T. Polymer 2001, 42, 9627.
9. Akio, S.; Hirokazu, N. Eur. Pat. 280297 (1988).
10. Eisuke, S.; Koichi, Y. Jpn. Pat. 2,003,306,586 (2003).
11. Tobita, E.; Urushibara, T.; Shimizu, T.; Kawamoto, N. Jpn. Pat. 2,003,335,968 (2003).
12. Jang, G. S.; Cho, W. J.; Ha, C. S. J Polym Sci B: Polym Phys 2001, 39, 1001.
13. Li, C. C.; Zhu, G.; Li, Z. Y. J Appl Polym Sci 2002, 83, 1069.
14. Jin, Y.; Hiltner, A.; Baer, E. J Appl Polym Sci 2007, 105, 3260.
15. Stephen, E.; Chantelle, E.; Markus, A. WO 98/29494, 1998.
16. Zhao, S. C.; Xin, Z. J Appl Polym Sci 2009, 112, 1471.
17. Caze, C.; Devaux, E.; Crespy, A.; Cavrot, J. P. Polymer 1997, 38, 497.
18. Jeziorny, A. Polymer 1978, 19, 1142.
19. Ozawa, T. Polymer 1971, 12, 150.
20. Liu, T. X.; Mo, Z. S.; Wang, S. E.; Zhang, H. F. Polym Eng Sci 1997, 37, 568.
21. Avrami, M. J Chem Phys 1939, 7, 1183.
22. Avrami, M. J Chem Phys 1940, 8, 212.
23. Kim, P. C.; Gan, S. N.; Chee, K. K. Polymer 1999, 40, 253.